IN-SITU, REAL-TIME MONITORING OF MECHANICAL AND CHEMICAL STRUCTURE CHANGES IN A V_2O_5 BATTERY ELECTRODE USING A MEMS OPTICAL SENSOR

H. Jung[1], K. Gerasopoulos[1], M. Gnerlich[1], A. Talin[2], and R. Ghodssi[1]*
[1]Department of Electrical and Computer Engineering, University of Maryland, College Park, Maryland, USA
[2]Sandia National Laboratories, Livermore, California, USA

ABSTRACT

This work presents the first demonstration of a MEMS optical sensor for *in-situ*, real-time monitoring of both mechanical and chemical structure evolutions in a V_2O_5 lithium-ion battery (LIB) cathode during battery operation. A reflective membrane forms one side of a Fabry-Perot (FP) interferometer, while the other side is coated with V_2O_5 and exposed to electrolyte in a half-cell LIB. Using one microscope and two laser sources, both the induced membrane deflection and the corresponding Raman intensity changes are observed during lithium cycling. Results are in good agreement with the expected mechanical behavior and disorder change of the V_2O_5 layers, highlighting the significant potential of MEMS as enabling tools for advanced scientific investigations.

INTRODUCTION

Capacity fading due to electrode mechanical and chemical structure changes during electrochemical cycling is a major limiting factor in battery cycle life. Continuous volume change and phase transformations are induced as Li-ions are inserted into and extracted from the electrodes which lead to gradual degradation of the battery performance [1, 2]. However, these mechanical and chemical structure changes are inherently coupled and most analysis techniques such as scanning electron microscopy, transmission electron microscopy and atomic force microscopy typically rely on post-operation inspection of the electrode. The aforementioned methods also can typically evaluate one parameter at a time (mechanical or chemical structure) only using bulky equipment in complex electrochemical apparatuses [3-5]. There is a need for *in-situ* monitoring platforms capable of providing simultaneous information on mechanical and chemical structure evolutions during battery operation in a simple and a reliable fashion.

Recently, several *in-situ* analysis techniques have been used in order to understand the mechanical evolutions in LIB electrodes. Among these, a multi-beam optical sensor (MOS) technique has proven to be an effective method for *in-situ* measurements of the mechanical properties in silicon thin-film electrodes during lithium cycling [6, 7]. In the MOS method, a substrate wafer is coated with a silicon oxide barrier layer, copper current collector and thin-film silicon active battery material. The substrate wafer is assembled into a customized electrochemical cell during electrochemical measurements. An array of parallel laser beams illuminates the substrate wafer surface. Curvature changes of the wafer induced by the stress generated in the silicon film due to lithium insertion/extraction are determined by measuring the relative change in the spacing between the reflected beams. This method provides quantitative information regarding the stress evolutions and bi-axial modulus changes in silicon electrode. However, the method is limited to providing the mechanical changes of the electrode but not the chemical structure changes.

In parallel, significant research has been focused on characterization of structural changes in LIB electrodes during electrochemical cycling. *In-situ* nuclear magnetic resonance (NMR) spectroscopy is used to study (de)alloying reactions of the silicon electrodes [8, 9]. This method provides insight into amorphous and amorphous-to-crystalline transformations that occur during the first and subsequent discharge-charge cycles. *In-situ* SEM/TEM techniques have also been utilized in order to investigate structural evolutions of silicon nanowires and nanoparticles. Direct observation of anisotropic expansion of the silicon nanowires has been reported by Liu et al [10] and sudden crystallization of $Li_{15}S_4$ phase during lithiation has also been observed with electron diffraction [11]. Nevertheless, these methods are restricted to providing only crystalline phase evolution of the electrodes during lithium cycling.

Here, we report a MEMS optical sensor device with important additional metrology functionalities as an *in-situ*, multi-modal sensing platform for monitoring of both mechanical and chemical structure changes of Li-ion battery electrodes in real-time. The V_2O_5 LIB electrode is used as a model system in this work.

DESIGN AND FABRICATION

Design

During battery operation, LIB electrodes experience continuous mechanical and chemical structure changes. The MEMS optical sensor platform is designed for monitoring these mechanical and chemical structure changes using FP interferometry and Raman spectroscopy, respectively. The principle of operation of the platform is shown in Figure 1.

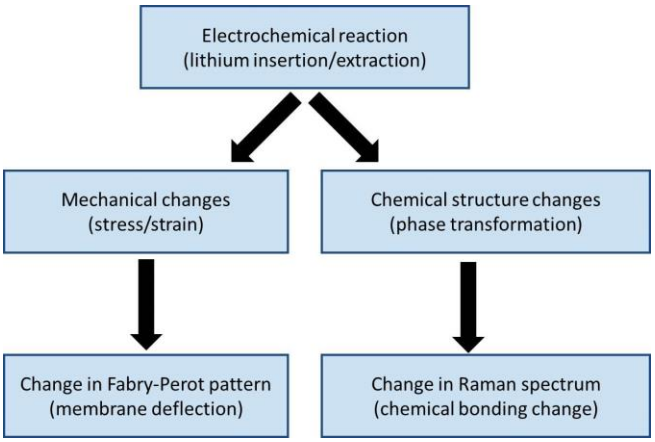

Figure 1: Schematic showing typical evolutions in LIB electrodes during battery operation and the changes recorded by the MEMS optical sensor platform.

The MEMS optical sensor consists of a flexible silicon nitride membrane which separates the device into two cavities (Figure 2(a)). The reflective surface of the membrane forms one side of a FP interferometer, while a bonded Pyrex wafer forms the second interference mirror. The other side of the membrane forms a battery cavity coated with the active battery material (V_2O_5). When the battery cavity is exposed to lithium-conducting electrolyte and metallic Li foil as a counter electrode, it forms a half-cell Li-ion

battery. During electrochemical operation, the V_2O_5 electrode expands and contracts as a result of Li-ion insertion/extraction. These volume changes cause deflection in the silicon nitride membrane. This mechanical change is monitored using FP interferometry. When the light reflects from the membrane and Pyrex glass, it produces an interference pattern. As the membrane deflects, the interference pattern also changes accordingly. These interference pattern changes are recorded and analyzed later for the mechanical change characterization. The chemical structure evolutions are also monitored using Raman spectroscopy, which can simultaneously probe the electrode surface through the partially reflective Pyrex glass and transparent films (Figure 2(b)).

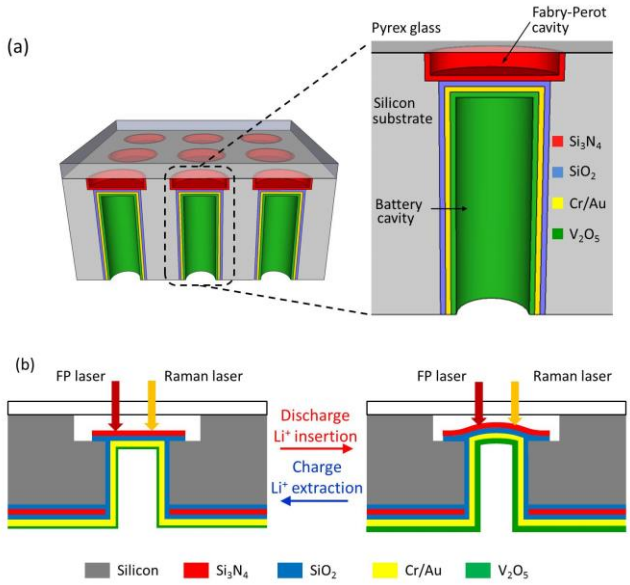

Figure 2: (a) 3D and cross-section diagrams of the MEMS optical sensor, (b) Schematic representation of the mechanical sensing mechanism principle.

Fabrication

The complete fabrication process is described in detail in our previous work [12] but will be briefly described here. A double-side polished silicon wafer is used as the substrate for the MEMS optical sensor fabrication. The FP cavity (12 µm deep) is etched using deep reactive-ion etching (DRIE) (Figure 3(a)). A 300 nm thick layer of SiO_2 is thermally grown followed by the deposition of a 700 nm thick layer of Si_3N_4 on both sides using low pressure chemical vapor deposition (LPCVD). Then, the Si_3N_4 and SiO_2 are masked with photoresist and etched using reactive-ion etching (RIE) from the FP cavity side. The battery cavity (488 µm deep) is formed by DRIE on the wafer backside, aided by a SiO_2 etch-stop layer (Figure 3(b)). The diameter of the battery cavities (150, 200, 250 and 300 µm) determine the diameter of the membranes. A Pyrex cap wafer is anodically bonded to form the optical FP cavity (Figure 3(c)). A SiO_2 passivation layer (50 nm) is deposited using plasma enhanced chemical vapor deposition (PECVD) in order to prevent Li-ion intercalation into the substrate. Subsequently, Cr/Au (5 nm/15 nm) thin films are deposited using sputtering to form the current collector. Finally, the battery cavity is coated with a thin-film V_2O_5 (135 nm) electrode using atomic layer deposition (ALD) (Figure 3(d)). The cross section SEM image of the fabricated MEMS optical sensor is shown in Figure 4. Upon finishing the fabrication process, the MEMS optical sensor device is packaged in a modified coin cell, routinely used in laboratories to test LIB electrodes, which is described in detail in our previous work [12].

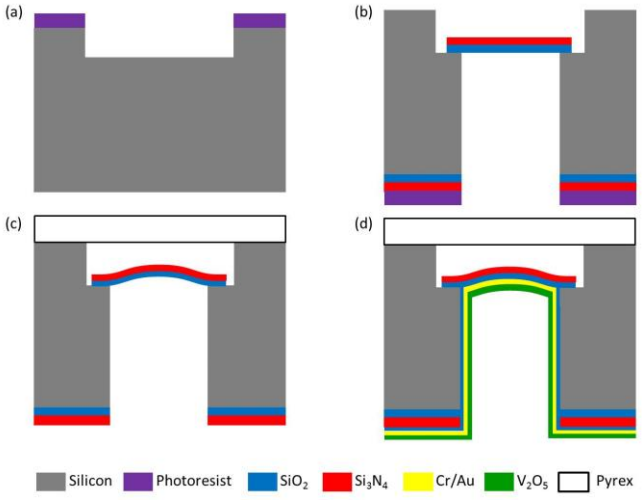

Figure 3: Schematic presentation of the fabrication process of the MEMS optical sensor.

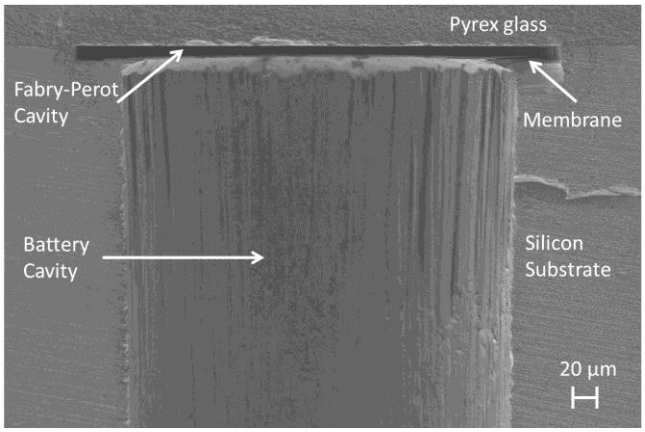

Figure 4: Cross-section SEM image of the MEMS optical sensor with a 300 µm diameter membrane.

EXPERIMENTAL SET-UP

The experimental set-up is a critical component of this work since it impacts the simultaneous monitoring of both mechanical and chemical structure evolutions of the electrode under test. A simplified schematic of the microscope set-up is shown in Figure 5. The white-light illumination source of the Raman microscope has been replaced with a despeckled red laser (638 nm) for measuring the membrane deflection by utilizing FP interferometry [13]. By employing an optical interferometric method, the same microscope used for the Raman spectroscopy analysis (Yvon Jobin LabRam ARAMIS, Horiba, Ltd.) can be modified to collect information on the membrane deflection, thus enabling multi-modal, real-time monitoring in a unified set-up. The red laser (638nm) illuminates

the FP cavity to produce an interference pattern, while the HeNe laser, 633nm is used as the excitation source for Raman spectroscopy measurements. A 10× objective is used to focus the Raman laser onto the electrode surface and the spectra are measured in back-scattering configuration. To avoid local heating of the electrode, the power of the laser beam is adjusted with a neutral density filter (0.9 W). Each spectrum is recorded for 60 seconds with only one accumulation.

The packaged device is connected to a potentiostat (VSP-300, BioLogic) and placed under an experimental set-up as shown in Figure 5. A Galvanostatic lithium cycling is conducted using the potentiostat in the voltage range of 2.8V - 3.5V with a current density of 2 μA/cm^2. All experiments were conducted in air under normal ambient conditions.

The imaging software installed on the computer connected to the Raman microscope supports automation function controlled by user specific operations programmed in JavaScript. This enables automatic switching between the two laser sources repeatedly throughout the experiment and computerized recording of the corresponding data. Two CCD cameras (labeled 1 and 2 in Figure 5) sequentially record the interference pattern (every 40 seconds) and the Raman spectra (every 220 seconds), respectively. The recorded interference pattern and Raman spectra are automatically saved in the computer and later correlated with the time stamped electrochemical data.

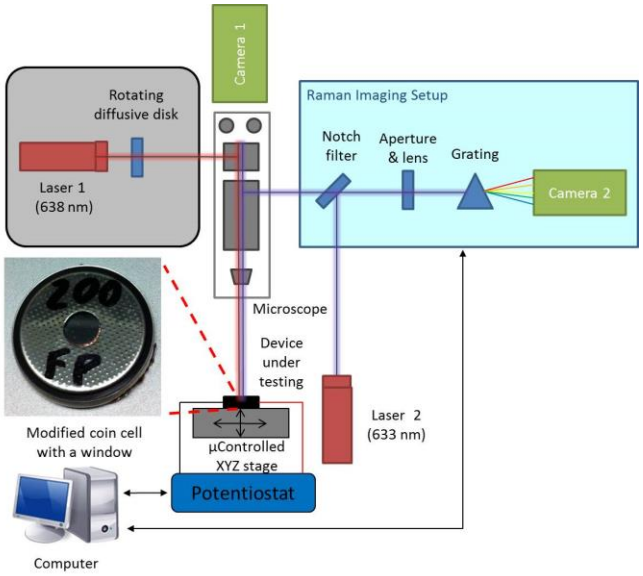

Figure 5: Simplified diagrams of the experimental setup showing the location of the device under test (face up) relative to the microscope.

RESULTS AND DISCUSSION

Changes in the FP interference pattern occur over long time scales since a single battery cycle may take several hours. Measurements in a single cycle can produce hundreds of images taken over hours. To analyze the data, a computerized image processing algorithm is developed using MATLAB. A detailed algorithm description can be found in our previous work [12]. According to the amount of lithium inserted into and extracted from the electrode, the radius of the FP interference pattern (fringe radius) changes due to the membrane deflection. The fringe radius is calculated based upon the comparison between the fringe radius of a pristine electrode and an electrode under electrochemical testing, as show in Figure 6.

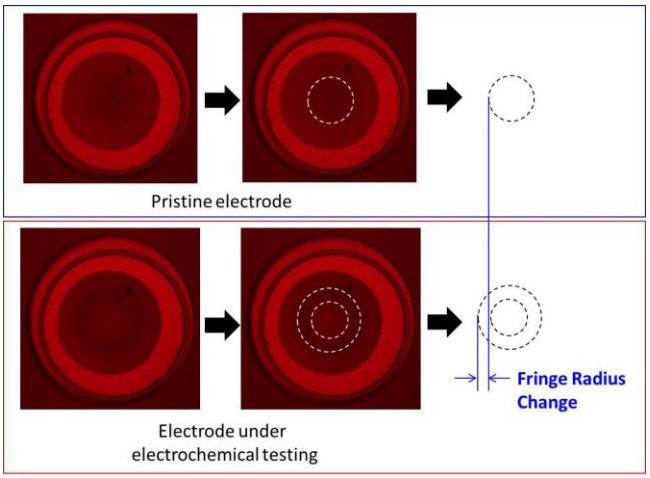

Figure 6: Photographs of the experimentally obtained interference pattern, showing relative fringe radius change.

The correlation between electrochemical data and changes in fringe radius for a membrane with 150 μm diameter during the second electrochemical cycle is shown in Figure 7. Upon lithium insertion (discharge), the V_2O_5 expands and the membrane deflects towards the Pyrex causing an increase in fringe radius. During lithium extraction (charge), the electrode contracts, the membrane deflects away from the Pyrex and the fringe radius returns closely to its original position. This indicates that the V_2O_5 electrode experiences irreversible volume changes during lithium cycling, which corresponds well with the results reported in literature [14]. Rapid increases and decreases in fringe radius are also observed during this process, and are attributed to the phase transition-induced (α, ε, and δ) volume changes in V_2O_5 with varying lithium content.

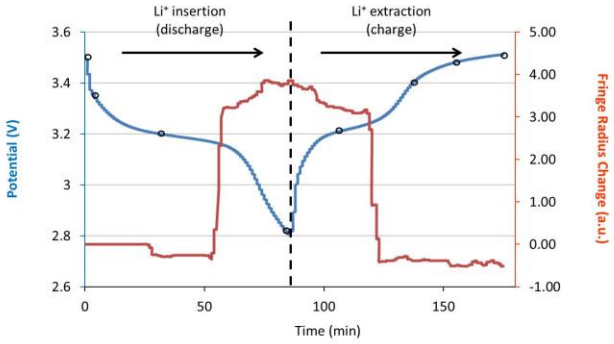

Figure 7: Discharge/charge and fringe radius change vs. time graphs

Simultaneously, the *in-situ* Raman spectra are collected and representative data at various points along the discharge/charge curve (black circles in Figure 7) are plotted in Figure 8. It has been

reported that the Raman intensity change at 145 cm^{-1} indicates the level of disorder between V_2O_5 layers [1]. As the level of disorder increases during lithium insertion, the Raman peak intensity at 145 cm^{-1} vanishes. On the other hand, the Raman peak at 145 cm^{-1} re-appears as lithium ions are extracted indicating which the V_2O_5 lattice is progressively recovered during lithium extraction.

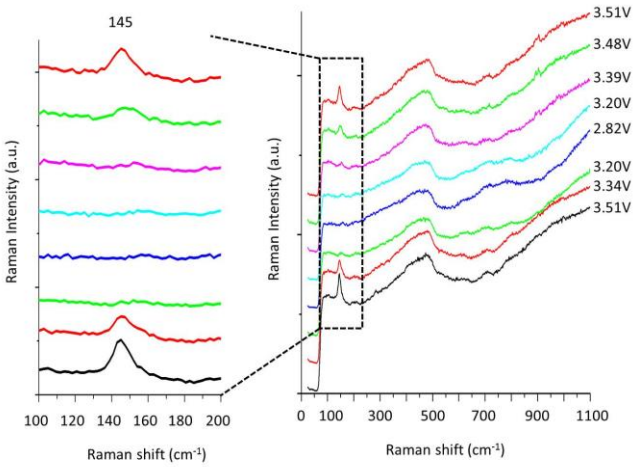

Figure 8: In-situ Raman spectra series at various potentials, highlighting the 145 cm^{-1} peak.

CONCLSION

The work presented here demonstrated the capability of *in-situ*, simultaneous monitoring of mechanical and chemical structure changes occurring in LIB electrodes for the first time.

The membrane deflection is induced by V_2O_5 thin film electrode volume expansion/contraction during electrochemical cycling. The FP interferometry is utilized in order to monitor the deflection of the membrane. At the same time, reversible changes in the level of disorder between the V_2O_5 layers is observed by the Raman spectra intensity change at 145 cm^{-1}. These mechanical and chemical structure changes are monitored simultaneously in a unified set-up using the MEMS optical sensor.

This multi-modal, *in-situ* monitoring technique can be utilized as a discovery platform for a wide variety of thin film LIB electrode materials and combinatorial material libraries of electrodes under test.

ACKNOWLEDGEMENTS

This work was supported by the Nanostructures for Electrical Energy Storage, an Energy Frontier Research Center funded by the U.S. Department of Energy (DOE), Office of Science, Office, Basic Energy Sciences (BES), under award number DESC0001160. The authors acknowledge the staff at Maryland Nanocenter.

REFERENCES

[1] R. Baddour-Hadjean, C. Navone, J.P. Pereira-Ramos, "*In situ* Raman microspectrometry investigation of electrochemical lithium intercalation into sputtered crystalline V_2O_5 thin films", Electrochimica Acta, 54, 6674 (2009).

[2] V.R. Armstrong, C. Lyness, P.M. Panchimatia, M.S. Islam, and P.G. Bruce, "The lithium intercalation process in the low-voltage lithium battery anode $Li_{1+x}V_{1-x}O_2$", Nature Materials, 10, 223 (2011).

[3] X.H. Liu, L. Zhong, S. Huang, S.X. Mao, T. Zhu, and J.Y. Huang, "Size-Dependent Fracture of Silicon Nanoparticles During Lithiation," ACS Nano, 6, 1522 (2012).

[4] L.Y. Beaulieu, V.K. Cumyn, K.W. Eberman, L.J. Krause, and J.R. Dahn, "A system for performing simultaneous *in situ* atomic force microscopy/optical microscopy measurements on electrode materials for lithium-ion batteries", Review of Scientific Instruments, 72, 3313 (2001).

[5] M.J. Chon, V.A. Sethuraman, A. McCormick, V. Srinivasan, and P.R. Guduru, "Real-Time Measurement of Stress and Damage Evolution during Initial Lithiation of Crystalline Silicon", Physical Review Letters, 107, 045503 (2011).

[6] V.A. Sethuraman, M.J. Chon, M. Shimshak, V. Srinivasan, and P.R. Guduru, "*In situ* measurements of stress evolution in silicon thin films during electrochemical lithiation and delithiation", Journal of Power Sources, 195, 5062 (2010).

[7] V.A. Sethuraman, M.J. Chon, M. Shimshak, N. Van Winkle, and P.R. Guduru, "*In situ* measurement of biaxial modulus of Si anode for Li-ion batteries", Electrochemistry Communications, 12, 1614 (2010).

[8] B. Key, R. Bhattacharyya, M. Morcrette,V. Seznec, J. Tarascon, and C.P. Grey, "Real-Time NMR Investigations of Structural Changes in Silicon Electrodes for Lithium-Ion Batteries", Journal of the American Chemical Society, 131, 9239 (2009).

[9] K. Ogata, E. Salager, C.J. Kerr, A.E. Fraser, C. Ducati, A.J. Morris, S. Hofmann, and C.P. Grey, "Revealing lithium–silicide phase transformations in nano-structured silicon-based lithium ion batteries via *in situ* NMR spectroscopy", Nature Communications, 5, 3217 (2014).

[10] X.H. Liu, H. Zheng, L. Zhong, S. Huan, K. Karki, L.Q. Zhang, Y. Liu, A. Kushima, W.T. Liang, J.W. Wang, J.H. Cho, E. Epstein, S.A. Dayeh, S.T. Picraux, T. Zhu, J. Li, J.P. Sullivan, J. Cumings, C.S. Wang, S.X. Mao, Z.Z. Ye, S.L. Zhang, and J.Y. Huang, "Anisotropic Swelling and Fracture of Silicon Nanowires during Lithiation", Nano Letters, 11, 3312 (2011).

[11] M.T. McDowella, S.W. Lee, C. Wang, and Y. Cui, "The effect of metallic coatings and crystallinity on the volume expansion of silicon during electrochemical lithiation/delithiation, Nano Energy, 1, 401 (2012).

[12] E. Pomerantseva, H. Jung, M. Gnerlich, S. Baron, K. Gerasopoulos, and R. Ghodssi, "A MEMS platform for *in situ*, real-time monitoring of electrochemically induced mechanical changes in lithium-ion battery electrodes", Journal of Micromechanics and Microengineering, 23, 114018 (2013).

[13] S.T. Koev, W.E. Bentley, and R. Ghodssi, "Interferometric readout of multiple cantilever sensors in liquid samples", Sensors and Actuators B: Chemical, B146, 245 (2010).

[14] J. Swiatowska-Mrowiecka, V. Maurice, L. Klein, and P. Marcus, "Nanostructural modifications of V_2O_5 thin films during Li intercalation studied in situ by AFM", Electrochemistry Communications, 9, 2448 (2007).

CONTACT

*R. Ghodssi, tel: +1-301-395-8158; ghodssi@umd.edu